



ELSEVIER

Thermochimica Acta 318 (1998) 251–263

thermochimica  
acta

## Stabilizing of aqueous kaolinite suspensions by thermal vapour-pressure shock explosion treatment

I. Lapides<sup>a,\*</sup>, S. Yariv<sup>a</sup>, N. Lahav<sup>b</sup>, M. Dvorachek<sup>c</sup>

<sup>a</sup> Department of Inorganic and Analytical Chemistry, The Hebrew University of Jerusalem, Jerusalem 91904, Israel

<sup>b</sup> The Seagram Center for Soils and Water Research, Faculty of Agriculture, The Hebrew University of Jerusalem, Rehovot 76100, Israel

<sup>c</sup> Geological Survey of Israel, Jerusalem 95501, Israel

Received 14 August 1997; accepted 17 October 1997

### Abstract

A new device for thermal vapor-pressure shock explosion (TSE) was constructed and the dispersion of three kaolinites (KGa-1, KGa-2 and S-5, well and poorly crystallized kaolinites from Georgia, USA and from Makhtesh Ramon, Israel, respectively) in aqueous suspensions investigated. In the new device, the clay suspension is heated in a sealed glass ampoule at 300°C for a few minutes and the water vapor pressure increases in the cell to  $\approx 100$  atm. At this stage the ampoule is shattered in ice-cold water. This treatment stabilized suspensions of KGa-1 and S-5 kaolinites. Particle-size distribution analysis showed that, by this treatment, smaller particles were obtained. A suspension of KGa-2 was not stabilized by this treatment although particles became smaller. Suspensions of the three kaolinites peptized by sodium pyrophosphate, were compared with those obtained by TSE treatment. SEM images and XRD patterns of sedimented films showed that tactoids became thinner as a result of the TSE treatment. EDS analysis of Ti suggested that the small particles, after the TSE treatment were formed from the disaggregation of the large aggregates. © 1998 Elsevier Science B.V.

**Keywords:** Aqueous clay suspension; Kaolinite; SEM images; Size dimensions; Thermal treatment; X-ray analysis

### 1. Introduction

Compared to other clay minerals, the surface area, surface charge and cation exchange capacity of kaolinite are relatively small. In addition, it has no inter-layer or zeolitic water. However, kaolinite can intercalate several inorganic salts and a variety of organic compounds, and the basal spacing expands from 0.715 nm to higher values [1]. Heller-Kallai [2] studied the effect of intercalation on the degree of order of kaolinites. They showed that the intercalation

of DMSO induced an increase of the disorder as revealed from the broadening of the X-ray peaks and a decrease in the Hinckley index after thermal de-intercalation of the DMSO.

In contrast to smectite clays, aqueous suspensions of most kaolinites are unstable, and peptizers such as sodium pyrophosphate (NaPP) or sodium carbonate are required to stabilize their suspensions [3]. The peptization results from the specific adsorption of the anionic species at the broken bonds, which reverses the positive edge charge into a negative one and, consequently, edge-to-face flocs are deflocculated [4].

\*Corresponding author. E-mail: isaak@vms.huji.ac.il

For most industrial applications kaolinite is ground and fine platelets with hexagonal shapes and large diameters are obtained by a mechanical delamination [3]. This process is accompanied by partial amorphisation of the kaolinite [5]. The purpose of the present investigation was to form stable aqueous suspensions of kaolinite without chemical treatments.

Recently, we reported on the application of a device for thermal vapour-pressure shock explosion (TSE) in which a clay mineral, palygorskite, was dispersed in an aqueous suspension [6]. Before the TSE treatment, palygorskite aqueous suspensions were unstable and particles <3 µm in diameter were not present. As a result of the TSE treatment, smaller particles were obtained and the dispersability of palygorskite was improved. SEM pictures showed that the aggregates of the clay needles were disintegrated.

The TSE device was made of two stainless-steel pressure cells connected by a valve. The upper cell could be heated by a resistance wire, whereas the lower cell was kept at room temperature. In the 'heating cell' clay and water were hermetically sealed and heated at 220°C for ca. 5 min. This thermal treatment was accompanied by a pressure increase inside the cell, resulting from the water vapour. Due to the high pressure inside the cell, adsorbed water was not evolved from the clay at this high temperature. As soon as the valve was opened, the pressure inside the heating cell was released and the adsorbed water evolved. This shock led to a quasi-explosion of the clay particles due to the fast evolution of the interparticle water. A disruption of the aggregates resulted in smaller flocs and primary particles. The lower cell contained water to dilute the heated suspension and was named the 'dilution cell'.

In contrast to palygorskite, Georgia kaolinite, following the older version of the TSE treatment, did not form stable suspensions and did not show any decrease in particle size. In the present paper, the dispersion of three kaolinites is described by applying a new TSE version in which a glass ampoule is used as the heating cell. The temperature of the heating cell is 300°C and that of the dilution cell 0°C. In the new TSE device, the heated glass cell is shattered in the cold dilution cell and, consequently, the sudden release of pressure applied to the clay, together with the high temperature gradient, results in a shock explosion of the clay

particles stronger than the explosion obtained in the old TSE system.

## 2. Experimental

### 2.1. Materials

Two kaolinites from Georgia (USA), KGa-1 (well crystallized) and KGa-2 (poorly crystallized) [7] were supplied by Wards. A sedimentary kaolinite from Makhtesh Ramon, Israel (S-5) [8,9], was kindly donated by Dr. S. Shoval from the Open University (Tel Aviv). Na<sub>4</sub>P<sub>2</sub>O<sub>7</sub>·10H<sub>2</sub>O was supplied by Reidelde Haën AG. Deionized water with a pH of 5.5–6.0 was used.

### 2.2. The new TSE device

The furnace was made of a vertical heating tube. Under the furnace was the 'dilution cell', a beaker made of steel, containing water cooled by ice to 0°C. Inside the furnace was a copper tube with its lower end immersed in the ice-cold water. A sealed ampoule of Pyrex glass (0.4–0.5 mm thickness) of 5×1 cm was used as a heating cell. The ampoule contained 0.2 g clay and 2.0 ml water. It was introduced into the copper tube and connected with a steel wire to a support on the tube. It was heated to 310°C (Fig. 1). Upon reaching the required temperature, the wire was released from the support, and the hot glass ampoule fell into the ice-cold water in the dilution cell and was shattered. The dilution cell, which contained the clay suspension, together with non-dispersed clay and glass fragments from the shattered ampoule, was transferred to a glass beaker. After 1 h, the suspension was separated from the glass fragments and the non-dispersed mineral fraction and transferred into a graduated cylinder. For the study of the properties of the TSE treated kaolinite suspensions, samples were collected from three parallel explosion experiments and the volume of the suspension was made up to 65 ml. Because the system is not hermetically isolated, the total amount of kaolinite which was collected under these conditions was ca. 80% of the initial material. Preliminary experiments showed that, in the absence of clay, an exploded ampoule did not form an aqueous suspension. It

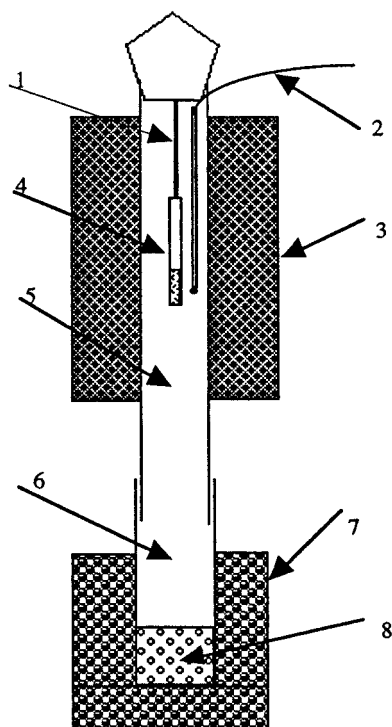


Fig. 1. A schematic presentation of a new version of the thermal vapour shock explosion (TSE) device: 1, steel wire; 2, thermocouple; 3, furnace; 4, glass ampoule; 5, heating tube; 6, dilution beaker; 7, ice thermostat; and 8, water.

should be noted that in this new TSE system, a water vapour pressure of ca. 100 atm was reached in the heated sealed ampoule and was followed by a fast release of the pressure.

### 2.3. Kaolinite treatments with Na-pyrophosphate

A sample of 1.0 g clay and 50.0 ml of 0.2% NaPP were stirred at room temperature for a duration of 12 h and then washed 5–6 times with 100 ml of deionized water.

### 2.4. Analysis of suspensions

Clay concentrations in the different suspensions were determined by evaporating 5 ml of suspension on a piece of polyethylene in air and weighing the solid residue.

The distribution of particle sizes in the range 0.5 to 60  $\mu\text{m}$  was measured in stirred suspensions of

untreated, and treated, kaolinites by a particle-size analyzer GALAI CIS-1 (computerized inspection system). The particle-size distributions in the 0–2  $\mu\text{m}$  range and the zeta potentials in the stable suspensions of the three NaPP treated samples and of the TSE treated KGa-1 and S-5 kaolinites in distilled water were determined by the particle-size analyzer Malvern-zetamaster (model ZEM). The measurement in the former instrument is performed while stirring the suspension, whereas in the latter instrument the suspension is at rest during the measurement. It was impossible to use the Malvern-zetamaster analyzer to obtain particle-distribution curves for the suspensions of untreated clays and of KGa-2 after the TSE treatment, because these suspensions were unstable. The particle-size distribution is given by the number of particles or their volume as a function of the particle size, calculated as spheres. The CIS-1 instrument also gives probability area density data as a function of the particle size.

### 2.5. Analysis of solids

Oriented samples for X-ray diffraction were obtained by drying suspensions on glass slides. To determine Hinckley's index [10], the dried samples were thoroughly ground and non-oriented powders were diffracted. X-ray diffractograms were recorded on a Philips automatic powder diffractometer (PW 1710) with a Cu tube anode. IR spectra of the same samples were recorded on a Bruker IFS 113v FT-IR spectrometer using KBr pellets.

SEM and energy dispersive spectroscopy (EDS) for chemical elements identification were carried out for local analyses of Ti, using JEOL-840 microscope and Link 10000 EDS. For this purpose, dried samples were coated with gold (ca. 200 Å). In the EDS analyses, each kaolinite particle was measured twice, with 8 and 18 kV electron beams. The 8 kV electron beam supplies data about the relative amounts of the elements at the surface of the particles, whereas the 18 kV beam, penetrates deeper and supplies this information on the elements inside the particles.

## 3. Results and discussion

The following terminology for kaolinite particle components (sub-particles) is used here. Primary

sub-particles are platelets of single tetrahedral–octahedral (TO) unit layers (fundamental particles) or tactoids. In the latter face-to-face interactions between several TO layers result in the formation of small clusters of parallel layers, stacked one above the other in the *c*-direction. Secondary sub-particles result from the aggregation of tactoids mainly by face-to-face or edge-to-face interactions, giving rise to book-house or card-house aggregates, respectively.

### 3.1. Dispersiveness of kaolinites

The suspensions of the TSE-treated kaolinite samples were collected in graduated cylinders. The sedimentation of KGa-2 particles is very fast even after the TSE treatment. Most of this kaolinite precipitates immediately, and after 2–5 h all particles were found at the bottom of the graduated cylinder. This is not so, however, for the kaolinites KGa-1 and S-5.

The suspension of KGa-1 after 30–40 h stratified to four layers with distinct boundaries and approximately similar heights. Similar behavior was obtained with TSE treated S-5, but in this case only three layers were obtained.

As one would expect, the concentration of the clay increased from the highest to the lowest layer. The stratification which was observed is due to sudden changes in the concentration of the clay with the height of the column, indicating that after an ageing period of 30–40 h the distribution of the particle size is in four or three groups in the suspensions of KGa-1 and S-5, respectively. In contrast to these suspensions, those of the NaPP treated clays did not show any stratification. It is possible that a secondary flocculation of the clay after the TSE treatment gave rise to this observation. After the NaPP treatment this flocculation does not occur and, consequently, stratification is not observed.

Values of the zeta potentials of the NaPP and TSE treated kaolinites were in the  $-24.0 \pm 3.0$  mV range. No significant differences between the different suspensions were observed.

Untreated KGa-1 and KGa-2 do not form stable aqueous suspensions. Untreated S-5 forms an aqueous suspension with a limited stability. Aqueous suspensions of NaPP treated KGa-1, KGa-2 and S-5 are stable even after thoroughly washing of the solid phase from the excess phosphate. The data in Figs. 2–4 show

that, after NaPP treatment, large particles of all three kaolinites become small due to the peptization of the aggregated clay by the phosphate.

### 3.2. Size distributions of particles (GALAI CIS-1 and Malvern-zetamaster instruments)

Figs. 2–4 show the size distributions of the clay particles with diameters  $>0.5 \mu\text{m}$ , in the suspensions of KGa-1, KGa-2 and S-5, (a) before treatment, (b) after an NaPP treatment and (c) after a TSE treatment. Particle-size distributions are related to (1) number of particles, (2) volume (which is equivalent to mass) and (3) surface area, all described in percentages as functions of particle size. Statistical values which were determined from these curves are summarized in Table 1. These distribution curves were obtained with CIS-1. Distribution curves for particles with diameters from 0 to  $2.0 \mu\text{m}$  were determined with a Malvern-zetamaster instrument. The modes recorded in these curves are shown in Table 1.

The statistical parameters obtained from the volume density, using the CIS-1 instrument, seem to be the most reliable for the present study [11] since the many small particles which are not observed by the instrument ( $<0.5 \mu\text{m}$ ) consist of a very small mass fraction of the clay. The few big particles which are present in the suspensions make up most of the mass of the sample (compare distribution curves obtained from volume measurements with those obtained from numbers of particles).

The statistical parameters related to the volume densities of untreated clays show that, in general, KGa-1 and KGa-2 are very similar in particle-size distributions. In both samples the mean and median sizes are very similar (see Table 1). There is a smaller number of larger particles in KGa-2, relative to the total clay amount. S-5, on the other hand, differs from KGa-1 and KGa-2 in having smaller particles. Also the median size is smaller than the mean size. The presence of small particles in S-5 may explain why untreated S-5 is slightly dispersed.

The three statistical parameters become very small after both treatments showing that, in both treatments, the average particle size critically decreases. After both treatments, the mean and median values for each sample are equal, indicating that 50% of the particles have diameters smaller than those of the mean values.

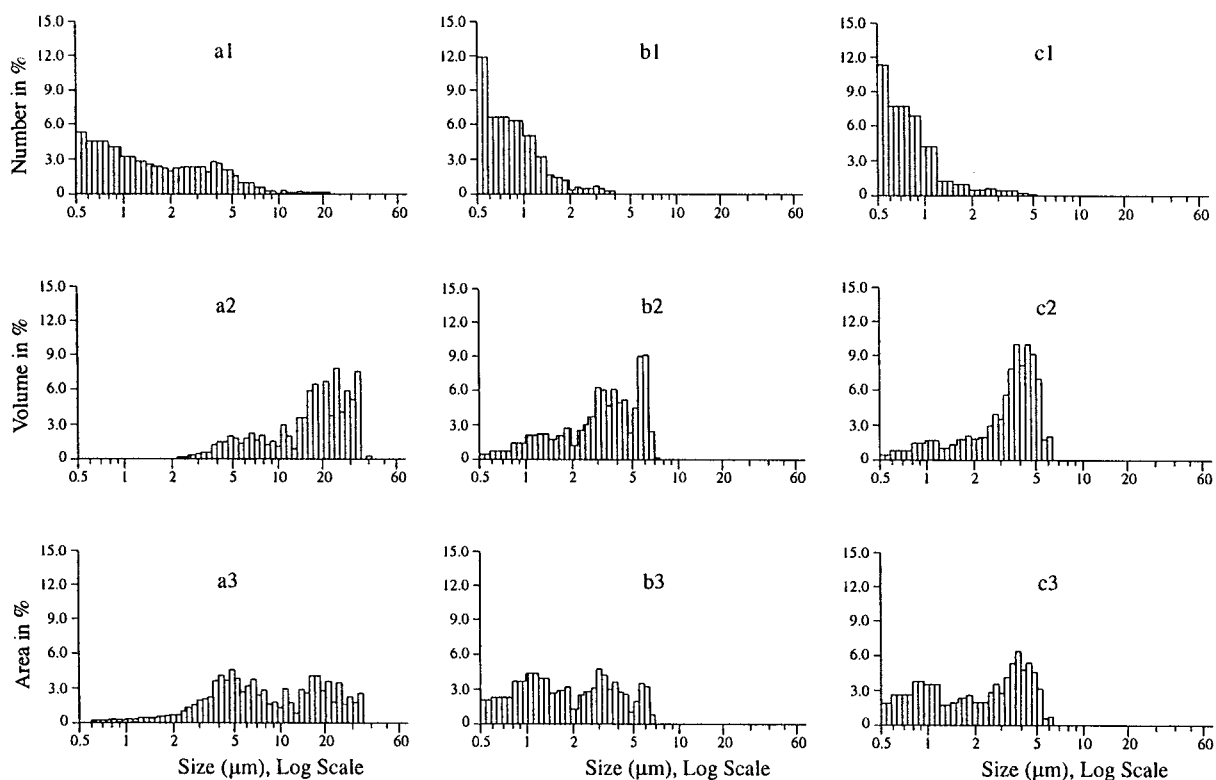


Fig. 2. Particle-size distribution curves of KGa-1 (GALAI – CIS-1,  $\mu\text{m}$ , log scale): (a) untreated kaolinite; (b) kaolinite after NaPP treatment; (c) kaolinite after TSE treatment; 1, number of particles in percentage (probability number density of particles) vs. size of particles; 2, volume of particles in percentage (probability volume density of particles) vs. size of particles; 3, surface area of particles in percentage (probability area density of particles) vs. size of particles.

Table 1

Statistical parameters (expressed in particle size,  $\mu\text{m}$ , CIS-1) determined from the distribution curves of KGa-1, KGa-2 and S-5 kaolinites before, and after, NaPP or TSE treatments

Sample	Probability number density			Probability volume density			Probability area density		
	mode	mean	median	mode	mean	median	mode	mean	median
<i>KGa-1</i>									
Untreated	0.55	2.18	1.26	23.99	17.78	17.40	4.86	10.93	7.22
NaPP treated	0.445 <sup>a</sup>	0.97	0.79	6.18	3.49	3.34	3.01	2.34	1.75
TSE treated	0.440 <sup>a</sup>	0.97	0.77	3.83	3.41	3.65	3.83	2.46	2.20
<i>KGa-2</i>									
Untreated	0.55	1.39	0.88	30.48	17.78	18.14	3.83	9.34	5.37
NaPP treated	0.450 <sup>a</sup>	0.74	0.68	4.86	2.65	2.86	0.90	1.54	0.92
TSE treated	0.55	0.94	0.75	5.27	3.58	3.65	3.53	2.39	1.79
<i>S-5</i>									
Untreated	0.55	1.03	0.79	17.43	8.15	6.16	3.53	3.83	2.52
NaPP treated	0.450 <sup>a</sup>	1.01	0.77	3.53	2.98	3.28	3.26	2.28	2.10
TSE treated	0.460 <sup>a</sup>	0.90	0.75	3.26	2.48	2.46	3.26	1.79	1.39

<sup>a</sup> Malvern-zetamaster instrument.

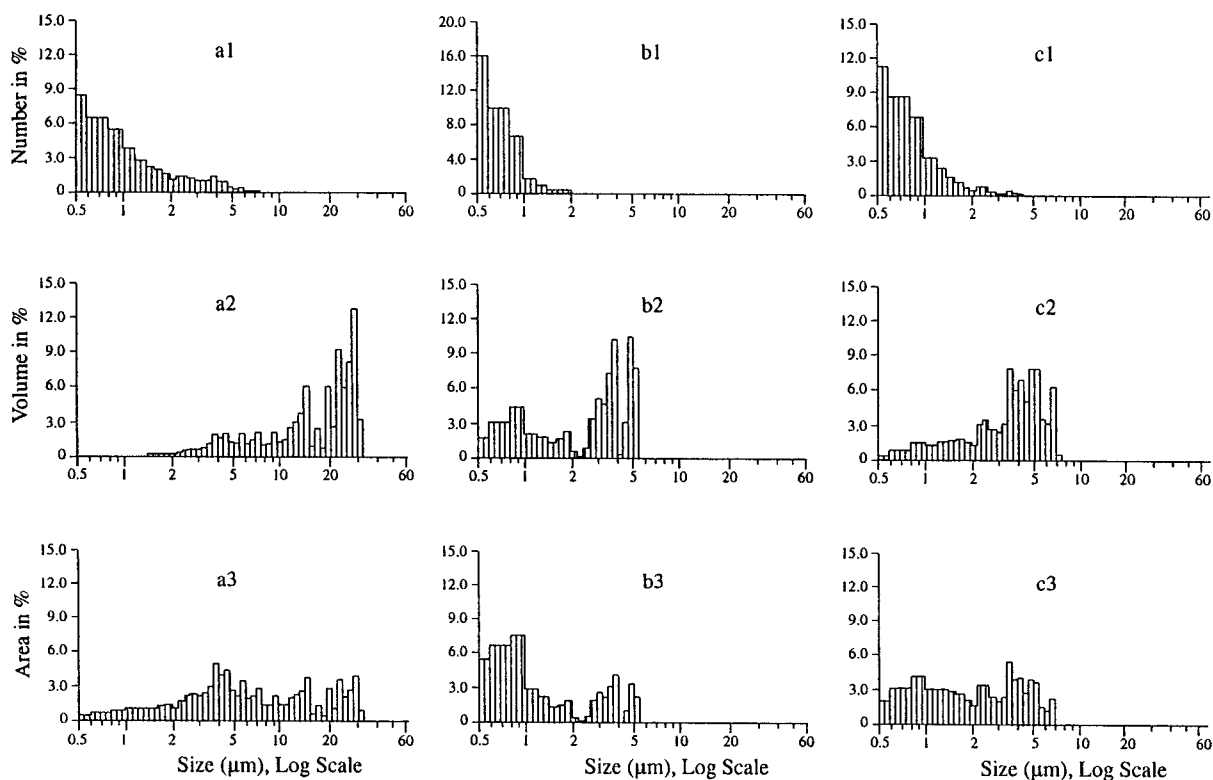


Fig. 3. Particle-size distribution curves of KGa-2 (GALAI – CIS-1,  $\mu\text{m}$ , log scale): The legend is the same as in Fig. 2.

The mean- and the median-size particles are always smaller than the mode-size particles. It should be noted that the number of large particles is very small.

The statistical parameters related to the number and area distributions are always lower than those obtained according to the volume density. Since, most of the particles (in number or area) have small sizes, they are not detected by the CIS-1 instrument and do not contribute to the statistical parameters of Table 1. From the fact that the parameters determined from the probabilities of number and area densities before treatment are always smaller than the parameters determined from the probabilities of volume density, it is obvious that small particles are already present to some extent before any treatment. The parameters determined from the probabilities of volume density before treatments in all three kaolinities indicate that very small particles are obtained after these treatments.

Similar effects of the NaPP and TSE treatments are shown in Figs. 2–4. Before the treatment, particles with diameters as large as 40, 35 and 19  $\mu\text{m}$  were detected in KGa-1, KGa-2 and S-5, respectively. After the NaPP treatment, the largest particles had diameters of 8, 5.5 and 5  $\mu\text{m}$  and, after the TSE treatment, they had diameters of 6.5, 7.5 and 4.8  $\mu\text{m}$ , respectively. As was mentioned in the experimental section, 20% of the solid clay was lost during the TSE treatment. This loss cannot account for the disappearance of these large particles after the treatment. The lost fraction may consist of large and small particles. From the distribution curves of untreated kaolinite, it was calculated that the mass of particles larger than those obtained after the TSE treatment makes up 80, 75, and 55% of the initial mass. But these amounts are much larger than the experimental loss ( $\approx 20\%$ ) which was determined by weighing the solid in samples before, and after, TSE treatments. This is an indication that most of the large particles were disrupted during the treat-

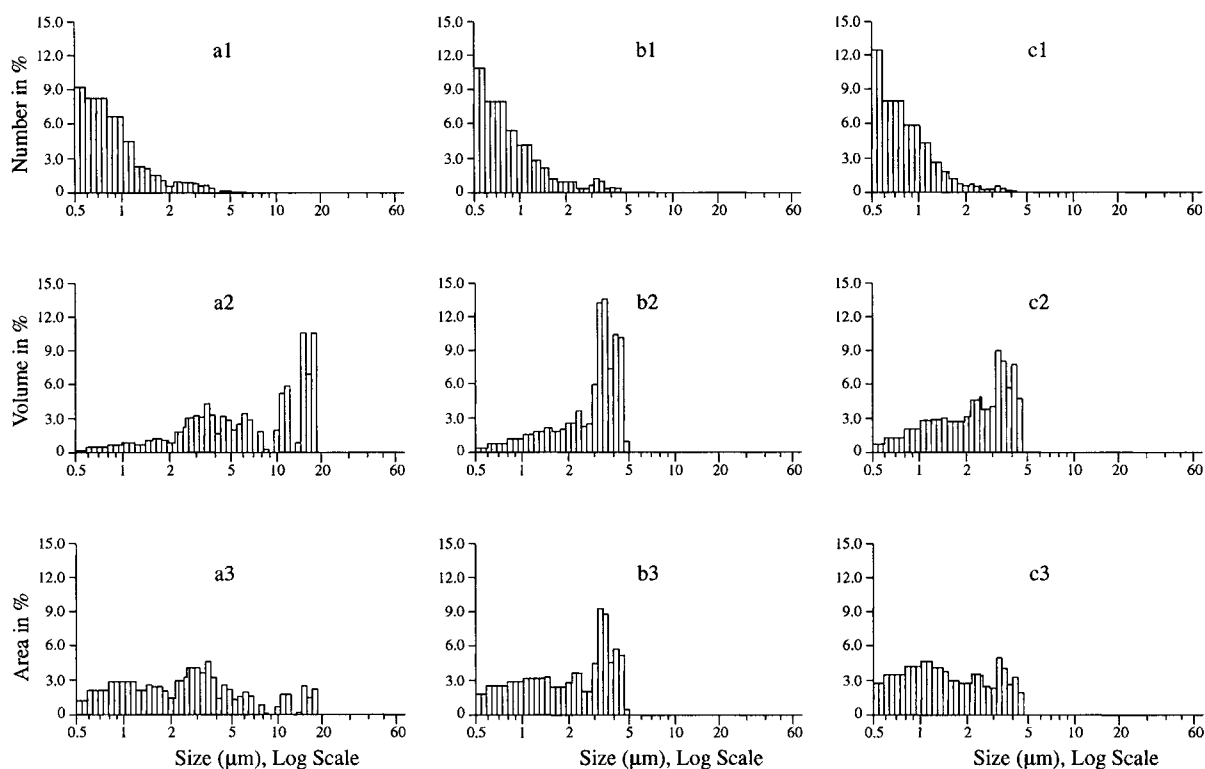


Fig. 4. Particle-size distribution curves of S-5 (GALAI – CIS-1,  $\mu\text{m}$ , log scale): The legend is the same as in Fig. 2.

ment and did not disappear due to the experimental loss.

The distribution curves which were obtained after the TSE or NaPP treatments showed that a diameter of  $\approx 2 \mu\text{m}$  divides the particles to two groups. The mass percentage of particles with a diameter larger than  $2 \mu\text{m}$  after TSE treatment are 75, 75 and 60, and after NaPP treatment 75, 60, and 75 for KGa-1, KGa-2 and S-5, respectively.

### 3.3. Scanning electron micrographs

Representative SEM pictures of the different kaolinities, untreated and after NaPP and TSE treatments, are shown in Figs. 5 and 6. All three untreated samples show many small particles composed of hexagonal layers, which are characteristic for kaolinite, and a few large particles. The presence of very small particles was also concluded from our statistical analysis in the previous section. The large particles of KGa-1 contain

aggregates (secondary sub-particles) composed of parallel primary sub-particles (tactoids) and have an elongated shape. The aggregate which is shown in Fig. 5(a and b) has the following dimensions:  $l=17 \mu\text{m}$ ,  $d=11.5 \mu\text{m}$  and the thickness of one tactoid  $0.3\text{--}0.5 \mu\text{m}$ . On the other hand, the large particles of KGa-2 form nearly spherical shapes and those of S-5 form flattened egg-like shapes. The aggregates which are shown in Fig. 6 have a diameter of  $15\text{--}30 \mu\text{m}$ . The differences in the shapes of the aggregates are associated with the differences in the sizes of the primary tactoids. As shown in Fig. 5(a) and Fig. 6(b and e), the diameters of most tactoids of KGa-1 are larger than those of KGa-2 and S-5. It is also obvious from these figures that the hexagons in KGa-2 and S-5 are highly distorted. The face-to-face interactions in KGa-1 are more significant than in KGa-2, whereas edge-to-face interactions are more significant in the latter kaolinite [12]. Concerning S-5, the SEM image shows that the diameters of the hexagons are variable and, conse-

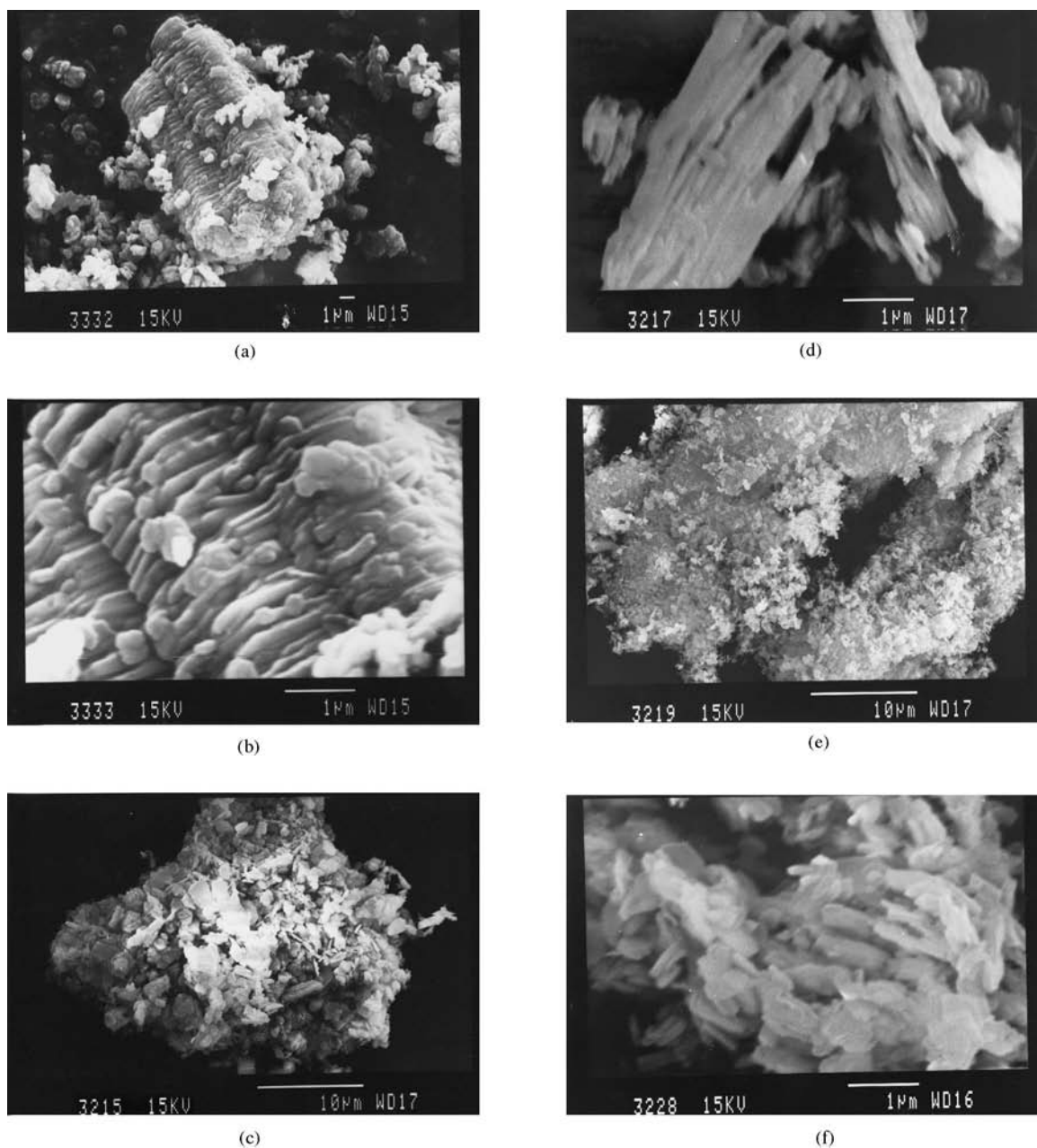


Fig. 5. SEM images of (a) and (b) untreated KGa-1; (c) and (d) KGa-1 after NaPP treatment; and (e) and (f) KGa-1 after TSE treatment.

quently, spherical aggregates are obtained mainly with face-to-face interactions between layers with parallel orientation (Fig. 6(d)).

The figures show that both treatments lead to the disruption of the clay aggregates. On comparing

Fig. 5(d) with Fig. 5(e), it is seen that the NaPP treatment leads to the appearance of small aggregates composed of several parallel tactoids, whereas the TSE treatment leads to the separation of the tactoids of the aggregates into thin entities.



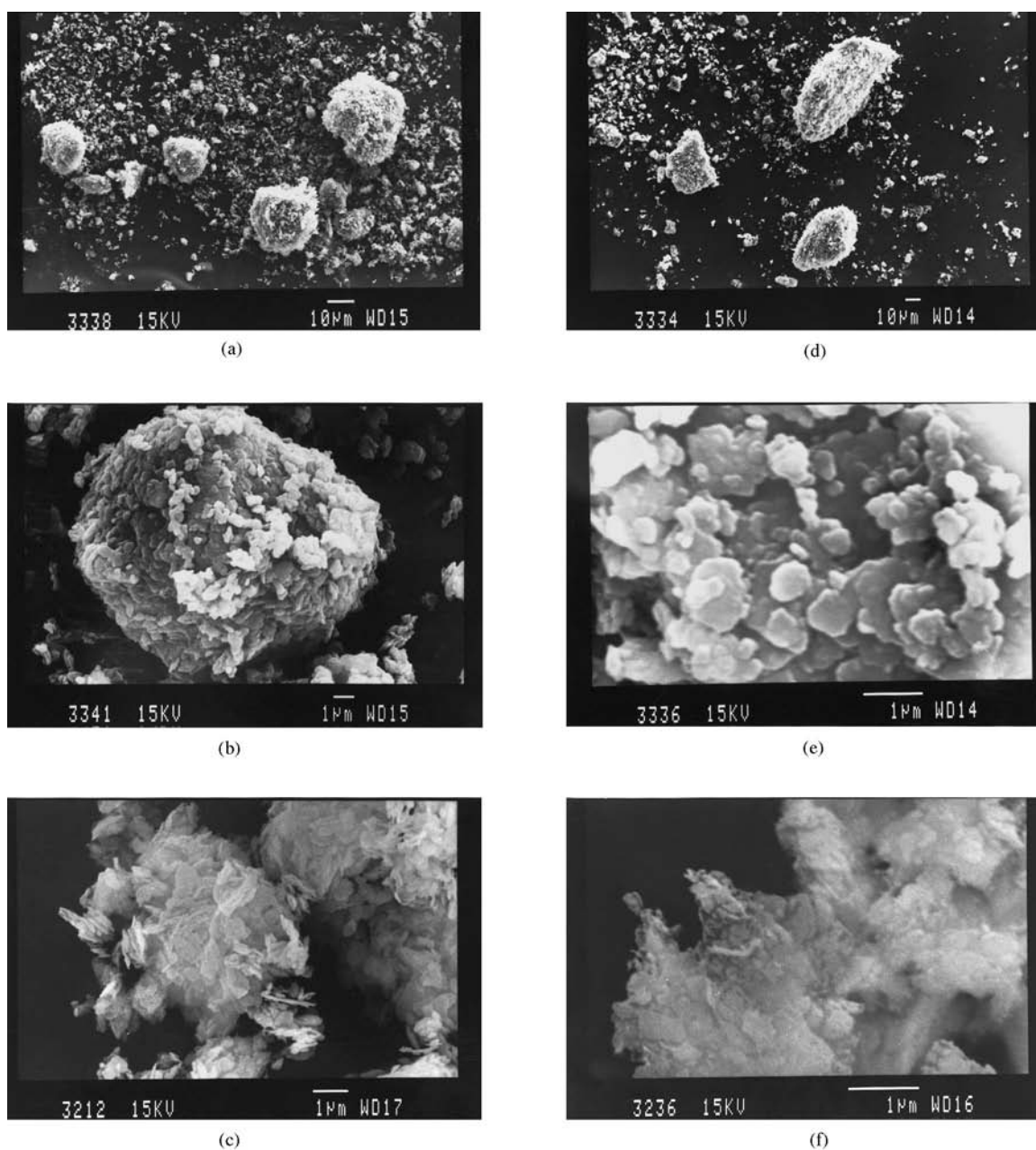


Fig. 6. SEM images of (a) and (b) untreated KGa-2; (c) KGa-2 after TSE treatment; (d) and (e) untreated S-5; and (f) S-5 after TSE treatment.

In the SEM pictures, we did not find any indication which shows that the diameter of the hexagon decreases after the TSE treatment. On the other hand, the tactoids appear thinner after this treatment. This is especially seen by comparing Fig. 6(d and e), and is in

agreement with the distribution curves which were constructed from surface areas. The percentages of the total surface area of particles with a diameter  $0.5 \mu\text{m}$  from total areas are ca. 0, 0.5 and 1.3% in untreated KGa-1, KGa-2 and S-5, respectively, and values

Table 2

Titanium contents in kaolinities from the literature ( $\text{TiO}_2$ , %) and from the EDS analysis (the number of pluses expresses the relative concentration of Ti)

Kaolinite	$\text{TiO}_2$	Untreated kaolinite				Treated kaolinite				TSE <sup>a</sup>	
		l.p. <sup>b</sup>		s.p. <sup>c</sup>		NaPP				8 kv	18 kv
		8 kv	18 kv	8 kv	18 kv	l.p. <sup>b</sup>	s.p. <sup>c</sup>	8 kv	18 kv		
										8 kv	18 kv
KGa-1	1.39 [7]	++	++	++	++	Tr <sup>d</sup>	++	—	—	Tr <sup>d</sup>	Tr <sup>d</sup>
TrKGa-2	2.08 [7]	+	+++	Tr <sup>d</sup>	Tr <sup>d</sup>	—	+++	+	++	Tr <sup>d</sup>	+
S-5	2.20 [8]	+	+++	—	—	Tr <sup>d</sup>	+++	—	++	++	++

<sup>a</sup> Contains mainly small particles.

<sup>b</sup> Large particles ( $\approx 20 \mu\text{m}$ ).

<sup>c</sup> Small particles ( $\approx 1.0 \mu\text{m}$ ).

<sup>d</sup> Traces.

increase to 2.0, 2.0 and 2.9% after the TSE treatment (Figs. 2–4).

### 3.4. EDS titanium analysis

Most kaolinities contain  $\text{TiO}_2$  in amounts between 0.06 and 3.54% [13]. Three varieties of Ti can be incorporated in the clay particles [14–18]: (1) amorphous  $\text{TiO}_2$ ; (2) microcrystals of rutile and anatase and (3) titanium isomorphically substituting octahedral aluminium in the kaolinite framework.

The EDS analyses of Ti in the three samples before, and after, treatments in small and large particles are summarized in Table 2. The relative amounts of Ti are indicated by plus symbols. The results which are discussed here, were obtained for the same particles shown in the SEM images which were discussed in the previous section (Figs. 5 and 6). The 18 kV beam penetrates into the inner parts of each particle whereas the 8 kV beam penetrates only through an envelope around the particle. Inside a large particle, in addition to kaolinite sub-particles (tactoids and aggregates), sub-particles of crystalline and amorphous  $\text{TiO}_2$  are present. The envelope of large particles may contain amorphous  $\text{TiO}_2$ . Inside a small particle, only very small sub-particles of crystalline and amorphous  $\text{TiO}_2$  can be present between the kaolinite sub-particles.

The total amounts of  $\text{TiO}_2$  in the natural samples, as they appear in Table 2, are quoted from the literature [7,8]. There is a very good correlation between these percentages of  $\text{TiO}_2$  and the relative amounts of Ti which were found in our study in the large particles,

but not with those which were found in the small particles. The large particles comprise most of the mass of the kaolinite samples and, therefore, contain most of the Ti. The small particles of KGa-1 seem to have the same Ti content as the large particles, but the small particles of KGa-2 and S-5 are different in their Ti content. It appears that most of the Ti in KGa-2 and S-5 forms relatively large sub-particles and, therefore, can be present only in the large particles.

The following conclusions can be drawn about the NaPP treatment. The large particles which were found after the treatment, are similar in Ti content to the large particles which were present in the untreated clays. This may serve as an indication that these particles persist after the NaPP treatment. Before the treatment, the large particles contained considerable amounts of Ti covering their surfaces. This adsorbed Ti, which is probably amorphous, was replaced by the pyrophosphate anions. The small particles which are obtained after the treatment, differ in their Ti content from the natural samples. This may suggest that, after the treatment, new particles were obtained from the peptization of the natural clay.

The TSE treatment yielded mainly small particles. The results in Table 2 were obtained on these particles. The Ti content after the TSE treatment differs from that in the natural samples. Considerable amounts of Ti were found in S-5, smaller amounts in KGa-2 and only traces in KGa-1. This may suggest that the small particles, after the TSE treatment, are new and were obtained from the destruction of the large particles. Some of the Ti precipitated together

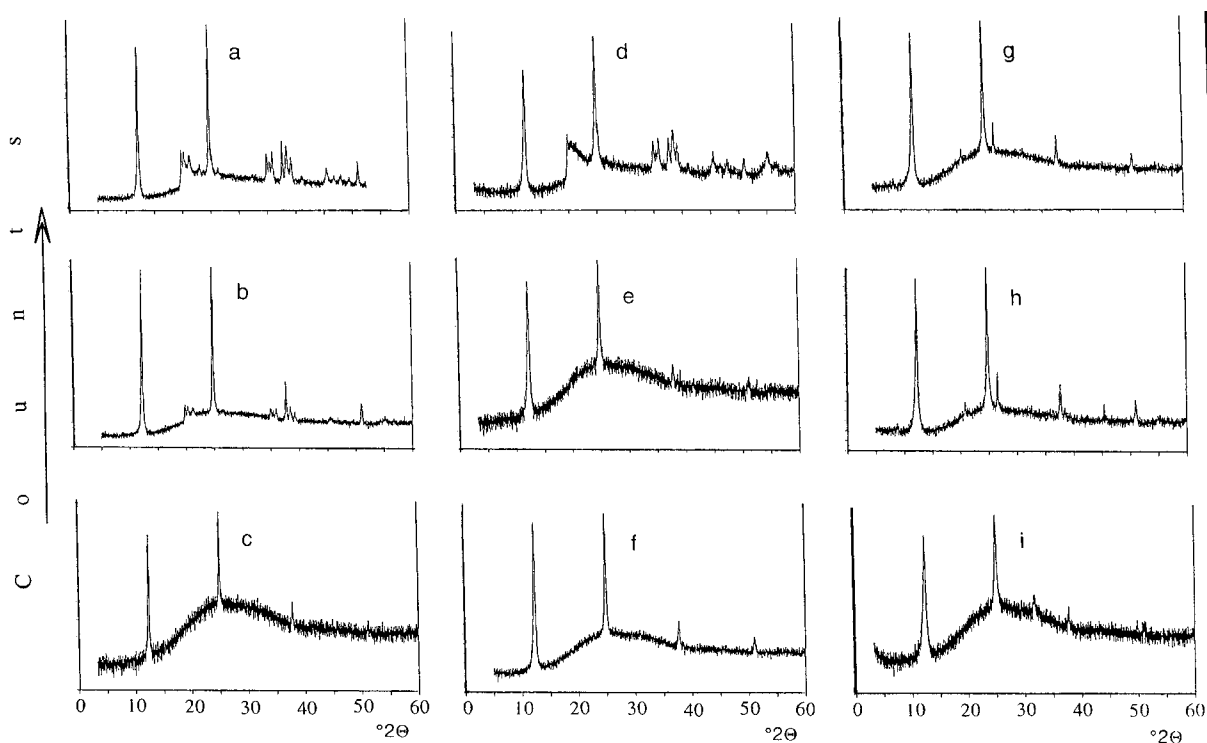


Fig. 7. X-ray diffractograms of sedimented films of kaolinites: (a) untreated KGa-1; (b) KGa-1 after NaPP treatment; (c) KGa-1 after TSE treatment; (d) untreated KGa-2; (e) KGa-2 after NaPP treatment (f) KGa-2 after TSE treatment; (g) untreated S-5; (h) S-5 after NaPP treatment; and (i) S-5 after TSE treatment.

with the shattered glass fragments because it formed large crystals which did not enter into the small clay particles.

### 3.5. XRD study

XRD of kaolinite films obtained by slow sedimentation from aqueous suspensions on glasses were recorded and representative diffractograms are shown in Fig. 7. The diffractograms of untreated KGa-1 and KGa-2 showed the presence of all  $hkl$  peaks, indicating that the sedimented films contain non-oriented kaolinite. However, the  $hk0$  peaks were weak relative to  $00l$  peaks, which indicates that some of the kaolinite in the film was oriented. In the case of KGa-1, the appearance of  $hkl$  is in agreement with the SEM image which showed book-house aggregates with  $l > d$ . It is expected that such particles will settle in a non-oriented fashion. In the case of KGa-2, the appearance of  $hkl$  is also in agreement with the SEM image which

showed card-house aggregates with no preferred orientation. Traces of quartz are also detected. The diffractogram of S-5 shows only  $00l$  peaks of the kaolinite and a small peak of quartz indicating that the sedimented film is composed of oriented layers. This is in agreement with the SEM image which showed that, in the aggregates, the layers, although of variable diameters, are parallel.

The diffractogram of KGa-1 after the NaPP treatment shows all  $hkl$  peaks, but the  $00l$  peaks are more intense. This indicates a partial orientation of the film by the treatment and is in agreement with the SEM image of this sample, which showed that the NaPP treatment leads to the appearance of small aggregates composed of several tactoids. The sedimentation of these aggregates is not necessarily with a preferred orientation. The diffractograms of NaPP treated KGa-2 and S-5 show only  $00l$  peaks. This is characteristic of a well-oriented sediment indicating that the suspended kaolinite particles were delaminated.

Table 3  
Effect of the treatments on Hinckley indexes [10] of kaolinites

Sample	Treatment		
	untreated	NaPP	TSE
KGa-1	0.94	1.12	1.05
KGa-2	0.41	0.50	0.55
S-5	1.03	1.12	1.03

The X-ray diffractograms of the sedimented films obtained from the three suspensions after the TSE treatment show only the 00 $l$  peaks. This is an indication that, as a result of the TSE treatment, the three kaolinites were delaminated. The TSE treated samples do not show the presence of quartz, which probably was separated together with the glass fragments.

XRD patterns of the three powder samples were traced before, and after, NaPP and TSE treatments and the Hinckley indices [10], which were determined on these non-oriented specimens, were used as criteria for changes in the disorder (Table 3). Changes of the Hinckley indices after the TSE treatment were negligible, showing that these treatment do not deform the packing of the kaolinite layers.

#### 4. Conclusions

A kaolinite, KGa-1, which does not give a stable aqueous suspension when using the old version of the TSE device, and S-5, which gives an aqueous suspension with limited stability without any treatment, form stable suspensions when the new version of the TSE is applied. In the new TSE version, the temperature difference between heating and cooling the sample is greater than in the old version and the release of pressure when the ampoule is shattered occurs more suddenly. Consequently, the explosion in the new TSE version is more effective, thus improving the dispersiveness of the clay.

Particle-size distribution analyses showed that most of the large particles were disrupted during a TSE treatment, and consequently, the average particle size critically decreases and also the largest particles in the suspension have shorter diameters.

These kaolinites give stable suspensions when they are peptized by NaPP. Here also, particle-size distribution analyses showed that the average particle size

critically decreases and the largest particles in the suspensions have shorter diameters. However, SEM images showed that NaPP treatment of KGa-1 leads to the appearance of small aggregates composed of several parallel tactoids, whereas the TSE treatment leads to the separation of the tactoids of the aggregates into their primary entities.

KGa-2 did not form stable suspensions after TSE treatment, although particles became small, with size distributions similar to those of KGa-1. No explanation for this observation was suggested. A stable suspension of KGa-2 is obtained in the presence of NaPP.

EDS analysis of Ti was used to get some information on the relations between the original large and small particles and the small particles which are obtained after the TSE treatment. Ti content in the latter differs from that in the original samples. This may suggest that the small particles, after the TSE treatment, are new and are obtained from the destruction of the large particles.

X-ray diffraction patterns of sedimented films after the TSE treatment showed only 00 $l$  peaks. This is characteristic of a well-oriented sediment, indicating that this treatment leads to the delamination of kaolinite.

There are almost no differences in the Hinckley indices before and after treatment, suggesting that the TSE treatment does not deform the packing of the kaolinite layers.

#### Acknowledgements

This research was supported by the Israel Council for Higher Education, Planning and Budgeting Committee. We thank Prof. Shlomo Magdassi from the Cassali Institute at the Hebrew University of Jerusalem for permission to use the particle-size Lazer Analyzers. Thanks are also due to Mrs. Frigitta Kahana for her assistance for the particle-size analyses.

#### References

- [1] A. Weiss, W. Thielepape, H. Orth, Proc. Intern. Clay Conf., Jerusalem 1 (1966) 277.

- [2] L. Heller-Kallai, *Clay Miner.* 26 (1991) 245.
- [3] H. van Olphen, *An Introduction to Clay Colloid Chemistry*. Interscience, New York, 1963.
- [4] P. Sennet, in: *Kirk–Othmer Encyclopedia of Chemical Technology*, vol. 6, 4th edn., Wiley, New York, 1992, p. 405.
- [5] S. Yariv, *Powder Technol.* 12 (1975) 131.
- [6] N. Lahav, D. Ovadyahu, A. Gutkin, E. Mastov, T. Menjeritzki, A. Adin, L. Rubinstein, D. Tropp, S. Yariv, *J. Thermal Anal.* 42 (1994) 67.
- [7] H. van Olphen, J.J. Fripiat, *Data Handbook for Clay Materials and Other Non-metallic Minerals*, Pergamon, Oxford, 1979.
- [8] Z. Minster, D. Shaked, A. Gur, *Isr. Geol. Soc. Ann. Meet.*, Mitzpe Ramon, 1987.
- [9] S. Shoval, M. Boudeulle, G. Panczer, S. Yariv, in: G. Baer, A. Heimann (Eds.), *Physics and Chemistry of Dykes*, Balkema, Rotterdam, 1995, p. 325.
- [10] D.N. Hinckley, *Clays Clay Miner.* 11 (1963) 229.
- [11] Atsuyuki Inoue, *Clay Sci.* 9 (1995) 259.
- [12] S. Yariv, H. Cross, *Geochemistry of Colloid Systems*, Springer-Verlag, Berlin, 1979.
- [13] A.C.D. Newman, G. Brown, *Chemistry of Clays and Clay Minerals*, Monograph No. 6, Mineralogical Society, London, 1987.
- [14] W.A. Deer, R.A. Howie, J. Zussman, *Rock-forming Minerals*, vol. 3, Wiley, New York, 1962.
- [15] D.L. Dolcater, J.K. Syers, M.L. Jackson, *Clays Clay Miner.* 18 (1970) 71.
- [16] M. Sayin, M.L. Jackson, *Clays Clay Miner.* 23 (1975) 437.
- [17] C.E. Weaver, *Clays Clay Miner.* 24 (1976) 215.
- [18] N. Malengreau, J.-P. Muller, G. Gallas, *Clays Clay Miner.* 43 (1995) 615.